Experimental Evidence of Conformational Differences between *C*-Glycosides and *O*-Glycosides in Solution and in the Protein-Bound State: The *C*-Lactose/*O*-Lactose Case

Juan-Félix Espinosa,[†] F. Javier Cañada,[†] Juan Luis Asensio,[†] Manuel Martín-Pastor,[†] Hansjörg Dietrich,[†,‡] Manuel Martín-Lomas,[†] Richard R. Schmidt,[‡] and Jesús Jiménez-Barbero*,[†]

Contribution from the Grupo de Carbohidratos, Instituto de Química Orgánica, CSIC, Juan de la Cierva 3, E-28006 Madrid, Spain, and Fakultät für Chemie der Universität Konstanz, Postfach 5560 M 725, D-78434 Konstanz, Germany

Received February 1, 1996[⊗]

Abstract: The conformational behavior of the synthetic glycosidase inhibitor *C*-lactose (**1**) has been studied in different solvents (water, *N*,*N*-dimethylformamide, dimethyl sulfoxide, pyridine) using NMR spectroscopy and molecular mechanics calculations. The obtained results have been compared to those previously obtained for its natural analogue, methyl α-lactoside (**2**). It is shown that the conformational behavior of *C*- and *O*-lactoses is only similar around the glycosidic bond, but not around the aglyconic bond. In addition, the extent of flexibility around the $\beta(1\rightarrow4)$ linkage is much larger for *C*-lactose (**1**) than for methyl α-lactoside, about 23% of the complete potential energy surface of **1** is appreciably populated, and several energy minima coexist in solution. The obtained results indicate that β-linked *C*-glycosides are fairly flexible compounds and that even variations of the solvent may heavily affect their conformational behavior. Finally, we report on the use of 2D transferred NOE experiments to study the recognition of *C*-lactose and its β-methyl derivative (**3**) by a galactose-binding protein, ricin-B. We also compare the obtained results to those reported for the complexation of regular lactose analogues. The experimental results unambiguously indicate that ricin-B selects different conformers of *C*-lactose (*anti* conformer) and its *O*-analogue (**2**) (*syn* conformer).

Introduction

Recent studies have demonstrated that oligosaccharides are involved in a number of recognition events such as cell adhesion, metastasis, and embryonic development, among others.[1] To play a role in these functions, the three-dimensional structure of the carbohydrate is of primary importance.[2] For an understanding of the mentioned events, natural compounds as well as structural analogues are usually required for biological testing. In this context, the search for new glycosidase inhibitors has led to a group of oligosaccharide analogues with the glycosidic oxygen substituted by carbon.[3] These carbon-bridged derivatives are thought to affect the activity of glycosidases, mainly *via* competitive inhibition,[4] and this general interest in *C*-disaccharides has recently led to various approaches to their synthesis.[5,6] Since a deeper understanding of the interaction of carbohydrates with proteins[7] requires detailed information on the conformational preferences of both species, the comparison of the conformational behavior of *C*-glycosides with the naturally occurring *O*-glycosides is a topic of interest.[6] Thus, it is important to determine whether the conformational characteristics of disaccharides are reflected in the carbon analogues. In a number of papers, and solely on the basis of a semiquantitative analysis of NMR data, mainly coupling constants, Kishi and co-workers[6] have postulated a similar conformation for both kinds of compounds. Nevertheless, the most usual method of establishing the solution conformation of oligosaccharides is the combination of NMR spectroscopy (NOE and *J* data) and molecular mechanics calculations.[8] On this basis, we now report on the conformational study of *C*-lactose (**1**; Figure 1) using NMR (quantitative *J* and NOE analysis) and MM3* [9] calculations. We compare these results with those obtained for methyl

[†] CSIC.

[‡] Universität Konstanz.

[⊗] Abstract published in *Advance ACS Abstracts,* October 1, 1996.

(1) (a) Phillips, M. L.; Nudelman, E.; Gaeta, F. C. A.; Perez, M.; Shingal, A. K.; Hakomori, S.; Paulson, J. C. *Science* **1990**, *250*, 1130−1133. (b) Halina, L.; Sharon, N. *Eur. J. Biochem.* **1993**, *218*, 1−27. (c) Harlan, J. M.; Liu, D. Y. *Adhesion: Its Role in Inflammatory Disease*; Freeman: New York, 1992. (d) Rademacher, T. W., Parekh, R. B.; Dwek, R. A. *Annu. Rev. Biochem.* **1988**, *57*, 785−823. (e) Lasky, L. *Annu. Rev. Biochem.* **1995**, *64*, 113−139.

(2) (a) Van Halbeek, H. *Curr. Opin. Struct. Biol.* **1994**, *4*, 697−709 and references therein. (b) Bock, K. *Pure Appl. Chem*. **1983**, *55*, 605−622. (c) Bush, C. A., *Curr. Opin. Struct. Biol*. **1992**, *2*, 655−660. (d) Bush, C. A.; Cagas, P. *Adv. Biophys. Chem*. **1992**, *2*, 149−180. (e) Rice, K. G.; Wu, P.; Brand, L.; Lee, Y.-C. *Curr. Opin. Struct. Biol*. **1993**, *3*, 669−674. (f) Woods, R. J. *Curr. Opin. Struc. Biol*. **1995**, *5*, 591−598.

(3) (a) Horton, D.; Wander, J. D. In *The Carbohydrates, Chemistry/Biochemistry*, 2nd ed.; Pigman, W., Horton, D., Eds.; Academic Press: New York, 1980; Vol. IB, p 803. (b) For a review, see: Postema, M. H. D. *Tetrahedron* **1992**, *48*, 8545−8599. (c) Wong, C.-H.; Halcomb, R. L.; Ichikawa, Y.; Kajimoto, T. *Angew. Chem., Int. Ed. Engl.* **1995**, *34*, 540. (d) *Chemistry of C-glycosides*; Levy, W., Chang, D., Eds.; Elsevier: Cambridge, 1995.

(4) Krohn, K.; Huns, H.; Wielckens, K. *J. Med. Chem.* **1992**, *35*, 511−517.

(5) (a) Dietrich, H.; Schmidt, R. R. *Liebigs Ann. Chem.* **1994**, 975−981 and references therein. (b) Dietrich, H.; Regele-Mayer, C.; Schmidt, R. R. *Carbohydr. Lett.* **1994**, *1*, 115−122. (c) Dietrich, H.; Schmidt, R. R. *Angew. Chem., Int. Ed. Engl.* **1991**, *30*, 1328−1329.

(6) (a) Wei, A.; Haudrechy, A.; Audin, C.; Hyuk-Sang, J.; Haudrechy-Bretel, N.; Kishi, Y. *J. Org. Chem.* **1995**, *60*, 2160−2169 and references therein. (b) Wang, Y.; Goekjian, P. G.; Ryckman, D. V.; Miller, W. H.; Babirad, S. A.; Kishi, Y. *J. Org. Chem.* **1992**, *57*, 482−489. (c) Wei, A.; Boy, K. M.; Kishi, Y. *J. Am. Chem. Soc.* **1995**, *117*, 9432−9437.

(7) (a) Quiocho, F. *Annu. Rev. Biochem*. **1986**, *55*, 287−315. (b) Bundle, D. R.; Young, N. M. *Curr. Opin. Struct. Biol.* **1992**, *2*, 655−660. (c) Vyas, N. K. *Curr. Opin. Struct. Biol.* **1991**, *1*, 732−740. (d) Bourne, Y.; van Tielbeurgh, H.; Cambillau, C. *Curr. Opin. Struct. Biol*. **1993**, *3*, 681−686. (e) Toone, E. *Curr. Opin. Struct. Biol.* **1994**, *4*, 719−728.

(8) For a detailed view of the application of molecular mechanics calculations to saccharide molecules, see: French, A. D.; Brady, J. W. *Computer Modelling of Carbohydrate Molecules*; ACS Symposium Series 430, American Chemical Society: Washington, DC, 1990.

S0002-7863(96)00346-0 CCC: $12.00

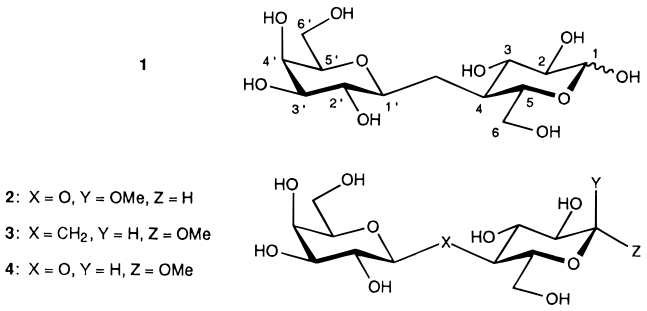

Figure 1. Views of compounds **1**−**4** showing the atomic numbering.

α-lactoside (**2**) using different force fields[10] in order to determine whether the conclusions derived from the conformational analysis of *C*-glycosides are appropriate for natural oligosaccharides as suggested by Kishi.[6] We have performed the conformational analysis both in water solution and in more apolar solvents (DMSO, DMF, pyridine) in order to obtain information about which factors determine the relative orientation of the glycosidic linkages.[11,12]

Finally, and to the best of our knowledge, it is not yet known whether both compounds are recognized by a carbohydrate-binding protein in the same conformation. Apart from the presence of the key interacting groups in the nonnatural substrate, this would be an essential requirement for an important inhibitory activity to occur. On this basis, we also report on the use of 2D transferred NOE (TR-NOESY) and transferred ROE (TR-ROESY) experiments[13] to study the complexation of *C*-lactose (**1**) and its *β*-methyl derivative (**3**) by a galactose-binding protein, ricin-B.[14] In addition, we compare the obtained results with those reported for the complexation of regular lactose analogues.[15,16] Taking advantage of the large size of lectins, TR-NOE (TR-ROE) experiments have recently been used to determine the 3D structure of protein-bound carbohydrates[17] and carbohydrate analogues[17f] by focusing on the easily detected NMR signals of the free ligand.

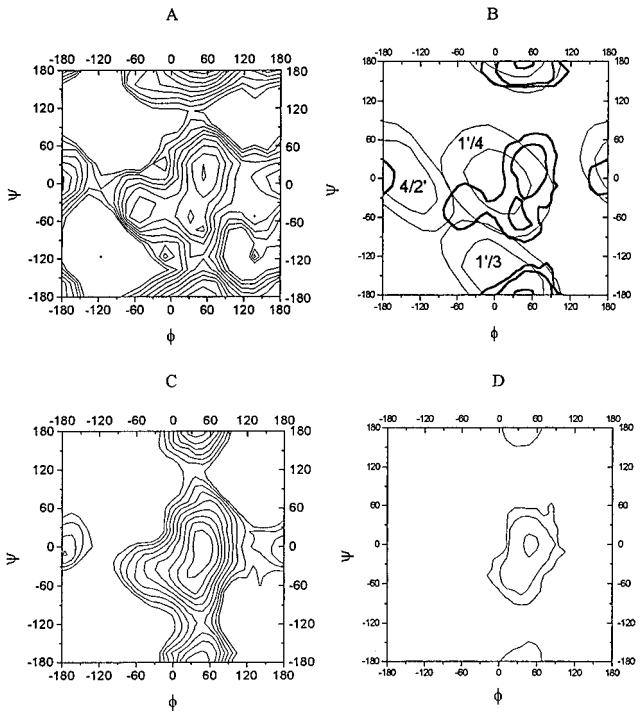

Figure 2. Adiabatic (a, c) and population distribution (b, d) maps for **1** (a, b) and **2** (c, d). Short interresidue distances of **1** and **2** are shown in map b. Energy contours are given every kcal/mol. Distribution contours are given at 10%, 1%, and 0.1% of the population. Distance contours are given at 2.5 and 3.0 Å.

Table 1. Torsion Angle Values (Φ,Ψ) of the Predicted Minima and Relative MM3* Populations of the Different Low-Energy Regions of Compound **1**[a]

	conformer (Φ, Ψ)				
	A (40, 180)	B (55, 20)	C (55, −70)	D (−55, −55)	E (180, 0)
pop (%)	54.0	31.6	9.3	3.3	1.7

[a] Φ and Ψ are rounded values.

Results and Discussion

Conformational Analysis of Isolated *C*-Lactose in D_2O Solution. Molecular Mechanics Calculations. The analysis of the 16 relaxed energy maps[8] (supporting information) calculated by MM3* [18] for **1** (Figure 2) indicated that the shapes of the surfaces are quite similar, independently of the initial configuration employed. Glycosidic torsion angles are defined as Φ (H1′−C1′−Cα−C4) and Ψ (C1′−Cα−C4−H4). The adiabatic surface built from the 16 relaxed maps is also shown in Figure 2. The minimization of the geometries included in the different valleys affords five minima below a steric energy level of 2 kcal/mol (Table 1). Figure 3 shows views of the main low-energy conformers of **1**. According to the probability distribution, 54% of the population is concentrated around the global minimum A (*anti*-type conformer). This region is defined by Φ values centered around 50° and Ψ values around 180°, occupying about 6% of the total area. A second broad low energy region exists around minima B and C (*syn*-type conformers), with 41% of the population, Φ values centered about 50°, and a variety of Ψ values ranging between −90° and +60°, occupying approximately 12% of the total area. The energy barrier between minima B and C is ca. 1 kcal/mol, and that between minima B and A is *ca.* 4 kcal/mol. The other two regions around conformers D and E are narrower and

(9) A preliminary communication has been reported: Espinosa, J. F.; Martín-Pastor, M.; Asensio, J. L.; Dietrich, H.; Martín-Lomas, M.; Schmidt, R. R.; Jiménez-Barbero, J. *Tetrahedron Lett.* **1995**, *36*, 6329−6332.

(10) (a) Asensio, J. L.; Jimenez-Barbero, J. *Biopolymers* **1995**, *35*, 55−73. (b) Asensio, J. L.; Martin-Pastor, M.; Jimenez-Barbero, J. *Int. J. Biol. Macromol.* **1995**, *17*, 137−148.

(11) (a) Lemieux, R. U. *Chem. Soc. Rev.* **1989**, *18*, 347−374. (b) Lemieux, R. U.; Bock, K.; Delbaere L. T. J.; Koto, S.; Rao, V. S. R. *Can. J. Chem.* **1980**, *58*, 631−653. (c) Woods, R. J., Edge, C. J.; Dwek, R. A. Modeling the Hydrogen Bond. *ACS Symp. Ser.* **1993**, *569*, 252−268.

(12) (a) Homans, S.; Rutherford, T. *Biochem. Soc. Trans.* **1993**, *21*, 449−452. (b) Perez, S. *Curr. Opin. Struct. Biol.* **1993**, *3*, 675−680. (c) Carver, J. P.; Michnick, S. W.; Imberty, A.; Cumming, D. A. *Ciba Found. Symp.* **1991** *158*, 6−26. (d) Hricovini, M., Shah, R. N; Carver, J. P. *Biochemistry* **1992**, *31*, 10018−10023. (f) Imberty, A.; Tran, V.; Perez, S. *J. Comput. Chem.* **1989**, *11*, 205−216.

(13) A preliminary communication was given: Espinosa, J. F.; Cañada, F. J.; Asensio, J. L.; Dietrich, H.; Martín-Lomas, M.; Schmidt, R. R.; Jiménez-Barbero, J. *Angew. Chem., Int. Ed. Engl.* **1996**, *35*, 303−306.

(14) . Olsnes, S.; Sandvig, K. In *Immunotoxins*; Frankel, A. E., Ed.; Kluwer Academic Publishers: Dordrecht, The Netherlands, 1988.

(15) Asensio, J. L.; Cañada, F. J.; Jimenez-Barbero, J. *Eur. J. Biochem.* **1995**, *233*, 618−630 .

(16) Bevilacqua, V. L.; Thomson, D. S.; Prestegard, J. H. *Biochemistry* **1990**, *29*, 5529−5537.

(17) (a) Weimar, T.; Peters, T. *Angew. Chem., Int. Ed. Engl.* **1994**, *33*, 88−91. (b) Bevilacqua, V. L.; Thomson, D. S.; Prestegard, J. H. *Biochemistry* **1992**, *31*, 9339−9349. (c) Bundle, D. R.; Baumann, H.; Brisson, J.-R.; Gagne, S. M.; Zdanov, A.; Cygler, M. *Biochemistry* **1994**, *33*, 5183−5192. (d) Glaudemans, C. P. J.; Lerner, L.; Daves, G. D.; Kovac, P.; Venable, R.; Bax, A. *Biochemistry* **1990**, *29*, 10906−10911. (e) Scheffler, K.; Ernst, B.; Katopodis, A.; Magnani, J. L.; Wang, W. T.; Weiseman, R.; Peters, T. *Angew. Chem., Int. Ed. Engl.* **1995**, *34*, 1841−1844. f) Andrews, J. S.; Weimar, T.; Frandsen, T. B.; Svensson, B.; Mario Pinto B. *J. Am. Chem. Soc.* **1995**, *117*, 10799−10804.

(18) Allinger, N. L.; Yuh, Y. H.; Lii, J. H. *J. Am. Chem. Soc.* **1989**, *111*, 8551−8562.

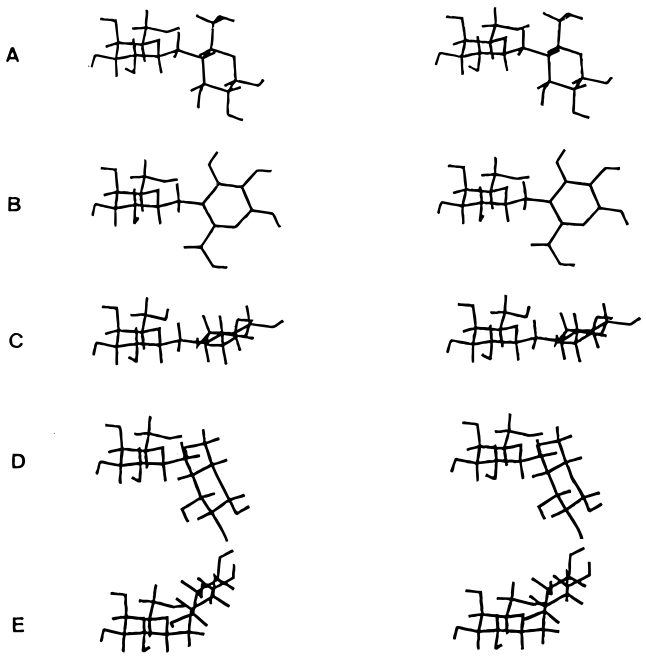

Figure 3. Stereo views of the low-energy conformations of **1**. From top to bottom: minimum A, Φ, Ψ, 36, 180, *anti;* minimum B, Φ, Ψ 54, 18, *syn*; minimum C, Φ, Ψ 54, −72; minimum D, Φ, Ψ −54, −54; minimum E, Φ, Ψ 180, 0.

account for an additional 5% of the surface. Minima A, B, C, and E are in agreement with the *exo*-anomeric effect,[19,20] accounting for 96.7% of the population. This represents the same conformational preference displayed by *O*-glycosides and agrees with Kishi's results,[6] and with the theoretical predictions of Houk.[21] However, the conformation around the *C*-aglyconic bond is rather different from that described by us for methyl α-lactoside (**2**).[10] For **2**, the central low-energy region (*syn*-type conformers) has a population of 97%, with only 3% of the population around minimum A (Figure 2). Therefore, MM3* calculations indicate that there are notable conformational differences between *C*-lactose and methyl α-lactoside. The previously reported structures for different $\beta(1\rightarrow4)$ equatorial linked disaccharides[22] are included in the low-energy region close to minima B and C. On the other hand, for **1**, the lowest energy region is defined by the same values of Φ, but Ψ values are about 180° and not around 0°. Besides, MM3* results indicate that the *C*-aglyconic bond is much more flexible than that of **2** since energy barriers are smaller, and ca. 23% of the complete Φ, Ψ potential energy surface is populated. On the other hand, the areas which are populated in the *O*-analogue **2** are only about 12%. As a further step, the conformational stability of the low-energy minima A and B was studied by MD simulations.[8,23] When the global minimum A (*anti*) was used as input, the trajectory remained (3 ns) in the corresponding low-energy region with barely no fluctuations in the sampled Φ and Ψ angles (supporting information). On the other hand, when the simulation used the conformer B (*syn*) as the starting point, interconversions from minimum B to minima C and D were observed. After 1.16 ns the trajectory went to minimum A and remained there (figure in the supporting information). Therefore, conformer A (*anti*) seems to be the most stable from a conformational point of view. The hydroxymethyl group of the glucose moiety shows transitions between the *gg* and *gt* conformations, while the galactose one moves between the *gt* and *tg* rotamers, as observed experimentally.[24]

Table 2. Experimental and Ensemble Average Calculated Steady State NOEs (Saturation Time 10 s) for **1** in D_2O Solution at 500 MHz[a]

	intensity (%)			intensity (%)	
proton pair	exptl	calcd	proton pair	exptl	calcd
H1′/H4	3.5	2.3	HproS/H5	1.6	2.1
H1′/(H3′ + H5′)[b]	14.8	15.1	HproS/H6a	1.0	1.1
H1′/H4′	−1.0	-0.9	HproS/H6b	1.0	0.6
H1′/H3	6.0	8.5	H4/H2′	1.0	0.3
H1′/H6b	*c*	0.8	H1′/HproS[d]	2.3	2.0
H1′/H5	1.0	0.9	HproR/H3	2.3	3.1
H1′/H6a	1.0	0.8	H1′/HproR[d]	1.0	0.1
HproR/H6b		0.5	HproR/H6a	2.7	2.2

[a] In all cases $\tau_c = 1.5 \times 10^{-10}$ s. NOEs of 1% are only approximated. The protocol for calculating the NOEs is given in the Experimental Section and has been deduced from an $\langle r^{-6}\rangle$ ensemble averaging. NOEs were also calculated from an $\langle r^{-3}\rangle$ ensemble averaging, producing basically the same results. NOEs are obtained by adding the contributions of both anomers. [b] H3′ and H5′ signals are close together; it is impossible to get an exact measurement of individual contributions. [c] Not determined. [d] ProR and proS assignments are based on NOE/*J* analysis and agree with the results published for similar compounds.[5b]

Table 3. Experimental and Calculated NOESY Intensities (Mixing Time 0.7 s) for **1** in D_2O at 500 MHz[a]

	intensity (%)			intensity (%)	
proton pair	exptl	ensemble av	proton pair	exptl	ensemble av
H1′/H3	5.9	7.5	HproR/H6a	4.1	4.2
H1′/H4	2.1	2.2	HproR/H3	5.7	4.6
HproS/H1′	4.6	6.3	H1′/HproS	2.3	2.6
H1′/(H3′ + H5′)	13.4	13.2	H4/H1′	1.8	1.6
H1′/HproR	<1	1.0	H4/H2′	1.0	<1

[a] In all cases $\tau_c = 0.15$ ns and the external relaxation is of 0.1 s^{-1}. The protocol for calculating the NOEs is given in the Experimental Section and has been deduced from an $\langle r^{-6}\rangle$ ensemble averaging. The NOEs were also calculated from a $\langle r^{-3}\rangle$ ensemble averaging, producing basically the same results.

Nuclear Magnetic Resonance Experiments. The validity of the calculations has been tested using measurements of vicinal coupling constants and NOEs.[25] The assignment of the resonances was made through a combination of COSY and HMQC (table in the supporting information). An important problem for the conformational analysis of the lactose type of disaccharides is that of strong overlap among H3, H4, H5, and in some cases H3′, nuclei with potential NOE to H1′. In our case, with a C atom instead of an O atom bridging the two rings, there is a shielding of H1′ and H4 resonances that no longer overlap with H3 or H5. The experimental NOEs are collected in Tables 2 and 3 and Figure 4. The most relevant interresidue proton−proton distances in terms of the glycosidic

(19) Lemieux, R. U.; Praly, J. P. *Can. J. Chem.* **1987**, *65*, 213−223.
(20) (a) Thatcher, G. R. J. *The Anomeric Effect and Associated Stereoelectronic Effects*; American Chemical Society: Washington, DC, 1993. (b) Tvaroska, I.; Bleha, T. *Adv. Carbohydr. Chem. Biochem.* **1989,** *47*, 45−123.
(21) Houk, K. N.; Eksterowicz, J. E.; Wu, Y.-D.; Fuglesang, C. D.; Mitchell, D. B. *J. Am. Chem. Soc.* **1993**, *115*, 4170−4177.
(22) (a) Hirotsu, K.; Shamada, A. *Bull. Chem. Soc. Jpn*. **1974**, *47*, 1872−1879. (b) Leeflang, B. R.; Vliegenthart, J. F. G.; Kroon-Batenburg, L. M. J.; van Eijck, B. P.; Kroon, J. *Carbohydr. Res*. **1992**, *230*, 41−61. (c) (d) Dowd, M. K.; French, A. D.; Reilly, P. J. *Carbohydr. Res*. **1992**, *233*, 15−36. (d) Kline, P. C.; Serianni, A. S.; Huang, S. G.; Hayes, M.; Barker, R. *Can. J. Chem.* **1990**, *69*, 2171−2182. (e) Engelsen, S. B.; Perez, S.; Braccini, I.; du Penhoat, C. H. *J. Comput. Chem.* **1995**, *16*, 1096−1107.
(23) (a) Homans, S. W. *Biochemistry* **1990**, *29*, 9110−9118. (b) Yan, Z.-Y.; Bush, C. A. *Biopolymers* **1990**, *29*, 799−811. (c) Hardy, B. J.; Sarko, A. *J. Comput. Chem.* **1993**, *7*, 831−847. (d) Brady, J. W.; Schmidt, R. K. *J. Phys. Chem.* **1993**, *97*, 958−966. (e) Kroon-Batenburg, L. M. J., Kroon, J., Leeflang, B. R., Vliegenthart, J. F. G. *Carbohydr. Res.* **1993**, *245*, 21−42.
(24) Bock. K.; Duus, J. Ø. *J. Carbohydr. Chem.* **1994**, *13*, 513−543.
(25) Neuhaus, D.; Williamson, M. P. *The Nuclear Overhauser Effect in Structural and Conformational Analysis;* VCH Publishers: New York, 1989.

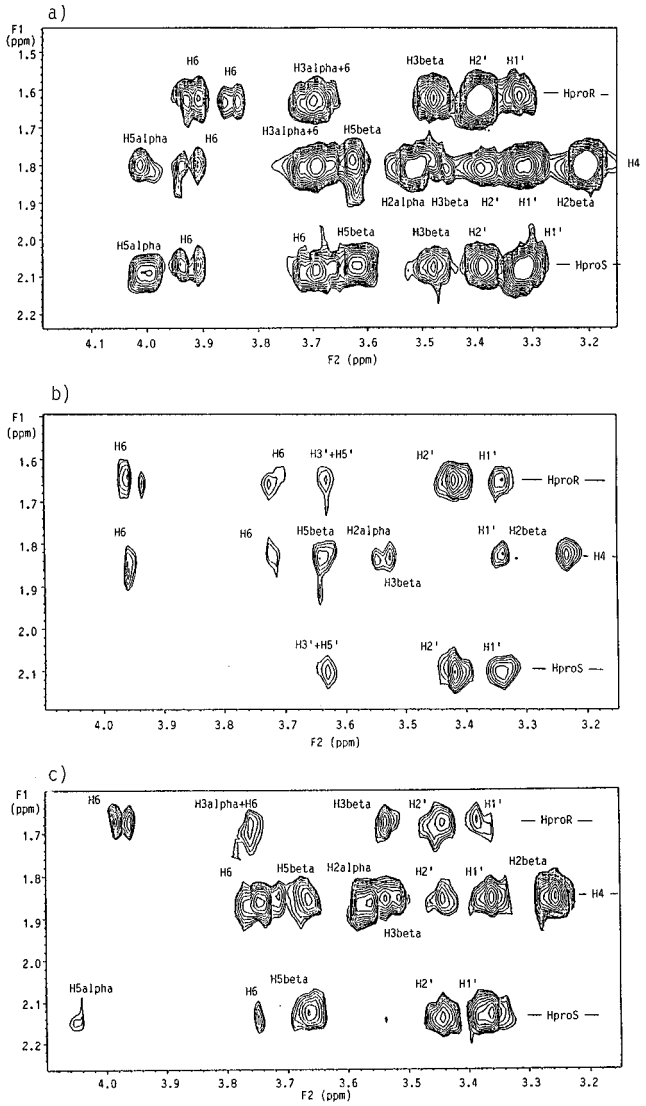

Figure 4. (a) Relevant NOEs for the HproR, HproS, and H4 protons of **1** in the 2D-NOESY ^{1}H-NMR spectrum (30 °C, D_2O, 500 MHz, mixing time 500 ms). (b) Relevant NOEs for the HproR, H-proS, and H4 protons of **1** in the 2D-TR-NOESY ^{1}H-NMR spectrum (Varian Unity, 500 MHz, 30 °C, D_2O) of **1** in the presence of ricin-B. Samples of ricin-B were concentrated after repeated cycles of exchange with deuterated sodium phosphate and transferred to the NMR tube to give a final pH of 6.5. A concentration of 0.12 mM and a molar ratio of *C*-lactose/ricin B of 20:1 were used. In this case, a mixing time of 300 ms was employed. TR-NOESY experiments were also carried out with mixing times of 120, 200, and 400 ms. (c) Relevant NOEs for the Hpro R, HproS, and H4 protons of **1** in the 2D-TR-ROESY ^{1}H-NMR spectrum (30 °C, D_2O, 500 MHz, mixing time 300 ms).

torsion angles are superimposed in the probability distribution maps, shown in Figure 2. The NOEs that unequivocally characterize these regions have been dubbed *exclusive NOEs*.[26] It can be observed that the H1′−H3 distance presents an intersection with the region around minimum A, and therefore the value of the NOE between these two protons will be sensitive to the population around this conformer. In an analogous manner the H1′/H4 NOE will be representative of the population around minima B and C. For methyl α-lactoside (**2**), the experimental interresidue H1′/H4 and H1′/H3 NOE values are 12.7% and 3.5%, respectively. However, for *C*-lactose, the corresponding relative values are now interchanged (the H1′/H3 NOE is now higher than the H1′/H4 NOE) and amount to 3.5% and 6.0%, respectively, in agreement with the conformational change predicted by the calculations. Nevertheless, the variation in the magnitude of the NOEs is dependent not only on the conformational changes but also on the different interproton distances, which are affected by the changes in the interglycosidic bonds and angles (C−C−C vs C−O−C). In addition, the global correlation time which produces the best fit between experimental and observed results for intraresidue proton pairs is somehow larger for *C*-lactose than for methyl α-lactoside (0.10 vs 0.15 ns). Nevertheless, and at least qualitatively, the existence of a stronger H1′/H3 NOE than that between H1′ and H4 implies that **1** spends most of its time in the region around minimum A than in the region around B. However, the presence of the H4/H2′ NOE indicates that the regions defined by conformers A−C are not the only two populated in water solution and that conformer E is also present. Tables 2 and 3 also show the experimental NOE values (from 1D and NOESY experiments), in comparison with those obtained from a relaxation matrix approach.[25] Both theoretical and experimental results indicate that the region around minimum A is the most populated in water. The experimental relevant coupling constant values of **1** are shown in Table 4 in comparison with the expected ensemble average values, calculated from the population distribution using the Karplus−Altona equation.[27] It can be observed that the matching is excellent and agrees with the conclusions of the NOE experiments.

Table 4. Vicinal Coupling Constants ($^3J_{H-H}$) across the C4−Cα−C1′ Bridge of compounds **1** and **3**

	$^3J_{H-H}$									
	a	*b*	*c*	*d*	*e*	*f*	*g*	*h*	*i*	*j*
H1′/HproS	1.2	1.6	2.4	2.4	2.2	1.0	1.4	0.9	11.5	5.0
H1′/HproR	10.3	10.3	9.2	8.7	10.2	10.8	11.3	10.0	3.2	1.9
H4/HproS	5.2	5.2	4.2	3.6	4.9	2.9	8.0	3.6	2.3	4.7
H4/HProR	3.5	3.7	4.2	4.2	4.2	4.0	1.7	12.2	12.3	4.3

[a] Experimental, 600 MHz in D_2O for **1**. [b] Experimental, 500 MHz in DMSO for **3**. [c] Experimental 500 MHz in DMF for **3**. [d] Experimental 500 MHz in Pyridine for **3**. [e] Ensemble average. [f] Theoretical from minimum A. [g] Theoretical from minimum B. [h] Theoretical from minimum C. [i] Theoretical from minimum D. [j] Theoretical from minimum E.

Therefore, the conformational behavior of *C*-lactose is well predicted by MM3*. Both theoretical and experimental results indicate that *C*-lactose adopts the *exo*-anomeric conformation around the *C*-glycosidic bond, like natural disaccharides, but the conformation around the *C*-aglyconic bond is rather different. In particular, minimum A (*anti*) is the most important for *C*-lactose, but the population around this minimum decreases considerably for methyl α-lactoside for which minima B and C (*syn*) dominate the distribution. Thus, minimum A seems to be more stable when the glycosidic O atom is replaced by carbon. Minimum A can be examined in both cases, at least as a first approximation, by focusing on through-space steric interactions, such as 1,3-diaxial-like destabilization.[6] Minimum A has only one 1,3-diaxial-like interaction between C4−C5 and C1′−O5′. Therefore, since the C−O distance is shorter than the C−C one, a possible explanation for the difference in stability in both cases could be that the 1,3-diaxial-like interaction is stronger for methyl α-lactoside than for *C*-lactose. Therefore, at least in this case, the conformational analysis of *C*-disaccharides is not directly applicable to natural oligosaccharides, in contrast with the conclusions of Kishi.[6] Also, the extent of flexibility around the $\beta(1\rightarrow4)$ linkage is much

(26) (a) Dabrowski, J.; Kozár, T.; Grosskurth, H.; Nifant'ev, N. E. *J. Am. Chem. Soc.* **1995**, *117*, 5534−5539. (b) Poppe, L.; von der Lieth, C. W.; Dabrowski, J. *J. Am. Chem. Soc.* **1990**, *112*, 7762−7771.

(27) Haasnoot, C. A. G.; de Leeuw, F. A. A. M.; Altona, C. *Tetrahedron* **1980**, *36*, 2783−2792.

larger for *C*-lactose (**1**) than for methyl α-lactoside. This fact implies that the loss of conformational entropy[28] for *C*-lactose will probably be higher than that for methyl α-lactoside upon binding to a protein receptor.

Conformational Features of Isolated *C*-Lactose in DMSO-d_6, DMF-d_6, and Pyridine Solutions. Oligosaccharide conformational analysis is sometimes performed in solvents different from water, such as DMSO[26] or even DMF,[29] since the presence of the water-exchangeable hydroxyl groups may allow the observation of additional NOEs, as well as the measurement of hydroxyl proton temperature coefficients, and even the observation of isotopic effects. On this basis, additional information on the existence of conformational flexibility for **1**, as well as a different conformational behavior with respect to **2**, was inferred from the dependence of the relevant NMR parameters on the solvent employed for the NMR measurements. In particular, the *β*-*O*-methyl *β*-glycoside analogue of **1** (**3**) was dissolved in three deuterated solvents, namely, DMSO, DMF, and pyridine, and after assignment of all the proton resonances (supporting information), the relevant interglycosidic coupling constants were obtained (Table 4). There were basically no differences among the temperature coefficients of the hydroxyl protons of **3** in each specific solvent. In fact, the coefficients were between 4.3 and 6.3 ppb in DMSO, between 6.7 and 9.0 ppb in DMF, and between 11.7 and 16.3 ppb in pyridine. The values indicate that no strong hydrogen bond was present in solution. In addition, all the vicinal coupling $^3J_{H-OH}$ values were around 6 Hz (figure in the supporting information), indicating that no preferred orientation around the C−O bonds was present. This result is in sharp contrast with that reported by us for methyl *β*-lactoside (**4**), the epimer of **2**.[30] In DMSO solution, HO(3) of **4** was shown to be intramolecularly hydrogen bonded, probably to O5′, since both a vicinal H3−C3−O3−H coupling constant smaller than 2 Hz and a rather small temperature coefficient (2 ppb) of this hydroxyl group were measured.[30] Furthermore, in the case of the *C*-glycoside analogue **3**, it can be observed that all the relevant coupling values (Table 4) around the glycosidic linkage indeed depend on the solvent. The trend is clearly shown when the polarity is decreased (from water to pyridine). Thus, $^3J_{H1'-HproS}$ and $^3J_{H4-HproR}$ values are higher in pyridine than in water, while $^3J_{H1'-HproR}$ and $^3J_{H4-HproS}$ values are significantly higher in D_2O solution than in pyridine. The measured values in DMSO and DMF are in between. The observed trend indicates that the population around conformer E (see Table 4) increases when the bulk dielectric constant is decreased. In fact, this behavior had been previously predicted by us[10] using the AMBER/Homans force field for the natural compound **2**. According to this force field, a significant stabilization of the corresponding conformer E at low dielectric constants is expected.[10] Additional indication of a higher amount of minimum E (*gauche*−*gauche*-type conformer, minimum E shows the Cα−C4 linkage *gauche* with respect to both C1′−O5′ and C1′−C2′ bonds) in the conformational distribution existing in DMF was deduced from the comparison of the ratios of the exclusive NOESY volumes (Figure 5) for the A (H1′/H3), B/C (H1′/H4), and E (H2′/H4)

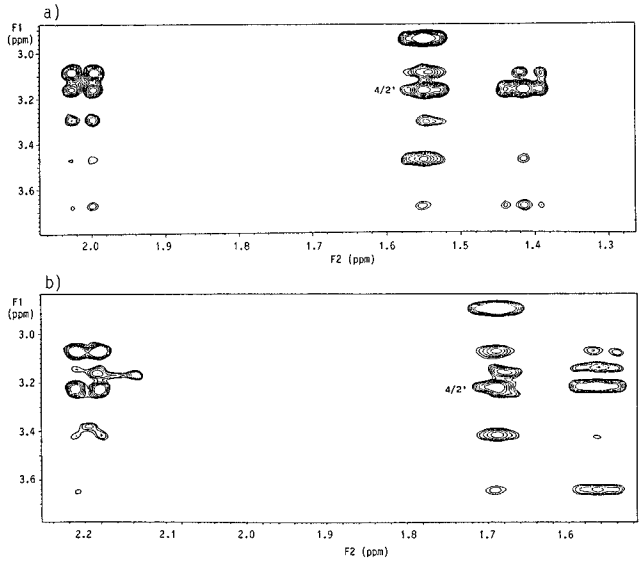

Figure 5. (Top) Section of the 2D-NOESY ^{1}H-NMR spectrum (Varian Unity 500 MHz, 30 °C, DMF) of **3**. In this case, a mixing time of 500 ms was used. The exclusive cross-peak for the *gauche*−*gauche* conformer is shown. (Bottom) Section of the 2D-NOESY ^{1}H-NMR spectrum (Varian Unity 500 MHz, 30 °C, DMSO) of **3**. In this case, a mixing time of 500 ms was used. The exclusive cross-peak for the *gauche*−*gauche* conformer is shown.

conformations. Although only a qualitative analysis was performed, it can be deduced that the (H1′/H3)/(H2′/H4) ratio, which corresponds to the A/E relative populations, substantially decreases on passing from D_2O (ratio 5.9) to DMF (ratio 2.7). In addition the (H1′/H4)/(H2′/H4) ratio, which accounts for the B/E relative populations also decreases from D_2O (ratio 2.0) to DMF (ratio 1.0). Both values indicate that the amount of conformer E is much higher in DMF than in water. From this qualitative analysis, it can be concluded that the conformational behavior of the *C*-glycoside, **3**, in nonaqueous solvents is also different from that of its corresponding *O*-analogue (**4**).[30] In addition, **3** shows a clear solvent-dependent conformational behavior, which indicates that the energy barriers among the different conformers existing in equilibrium are rather small (see below).[31,32]

The present results indicate that *β*-linked *C*-glycosides are fairly flexible compounds and that even variations of the solvent may heavily affect their conformational behavior. The conformational changes observed within this series also reflect the small energy barriers between the different energy regions, and therefore, conformations different from the major one existing in solution may be bound by the binding sites of lectins, antibodies, or enzymes.[33]

Conformational Analysis of *C*-Lactose and Methyl *β*-*C*-Lactoside When Bound to a Ricin-B Chain. For ligands which are not bound tightly and exchange with the free ligand at reasonably fast rates, the transferred nuclear Overhauser enhancement (TR-NOE) experiment, first proposed by Bothner-By,[34] and later developed by Albrand *et al*. and Clore and Gronenborn,[35] provides an adequate means to determine the

(28) Searle, M. S.; Williams, D. H. *J. Am. Chem. Soc.* **1992**, *114*, 10690−10697.

(29) (a) Yan, Z. Y.; Rao, B. N. N.; Bush, C. A. *J. Am. Chem. Soc.* **1987**, *109*, 7663−7669. (b) Rao, B. N. N.; Bush, C. A. *Carbohydr. Res.* **1988**, *180*, 111−128. (c) Poppe, L.; Dabrowski, J. *J. Am. Chem. Soc.* **1989**, *111*, 1510−1511.

(30) Rivera-Sagredo, A.; Jimenez-Barbero, J.; Martin-Lomas, M. *Carbohydr. Res.* **1991**, *221*, 37−47.

(31) Bock, K.; Duus, J. Ø.; Refn, S. *Carbohydr. Res.* **1994**, *253*, 51−67.

(32) Bernabe, M.; Fernandez-Mayoralas, A.; Jimenez-Barbero, J.; Martin-Lomas, M.; Rivera, A. *J. Chem. Soc., Perkin Trans. 2*, **1989**, 1867−1873.

(33) Imberty, A.; Bourne, Y.; Cambillau, C.; Rouge, P.; Perez, S. *Adv. Biophys. Chem.* **1993**, *3*, 71−118.

(34) Bothner-By, A. A.; Gassend, R. *Ann. N.Y. Acad. Sci.* **1972**, *222*, 668−676.

(35) (a) Albrand, J. P.; Birdsall, B.; Feeney, J.; Roberts, G. C. K.; Burgen, A. S. V. *Int. J. Biol. Macromol.* **1979***1*, 37−41. (b) Clore, G. M.; Gronenborn, A. M. *J. Magn. Reson.* **1982**, *48*, 402−417. (c) Clore, G. M.; Gronenborn, A. M. *J. Magn. Reson.* **1983**, *53*, 423−442. (d) For recent reviews, see: Campbell, A. P.; Sykes, B. D. *Annu. Rev. Biophys. Biomol. Struct.* **1993**, *22*, 99−122. (e) Ni, F. *Prog. NMR Spectrosc.* **1994**, *26*, 517−606.

Table 5. Experimental Normalized NOESY, TR-NOESY, ROESY, and TR-ROESY Intensities (%) That Characterize Each Conformation of **1** and **3** at 30 °C in D_2O at 500 MHz[a]

	intensity (%)				
proton pair	free **1** (NOESY)	bound **1** (TR-NOESY)	bound **3** (TR-NOESY)	free **1** (ROESY)	bound **1** (TR-ROESY)
H1′/H4	2.1	−1.2	−0.7	1.0	1.2
H1′/H3	5.9	−3.1	−2.5	2.4	7.1
HproR/H6[b]	5.1	−5.4	−4.9	2.0	4.7
H2′/H4	1.0	0.0	0.0	0.0	0.0
HproR/H3	5.7	0.0	0.0	1.2	1.4
HproS/H5	3.0	0.0	0.0	1.0	1.0
HproS/H6[b]	2.7	0.0	0.0	1.2	1.0

[a] The mixing times for the NOESY and TR-NOESY experiments were, respectively, 700 and 300 ms. Other mixing times were used additionally. The mixing time for ROESY and TR-ROESY was 150 ms in both cases. TR-ROESY experiments were also recorded with mixing times of 250 and 350 ms. [b] These NOEs are obtained by adding the contributions of both H6's.

conformation of the bound ligand. When the sugar and the protein are in fast exchange on the chemical shift scale, only a single set of averaged ligand resonances is observed (see supporting information), whose positions are approximately the same as those of the free sugar, under the experimental conditions used. When the molecular complex lies in the spin diffusion limit, $\omega\tau_c \gg 1$, cross-relaxation rates of the bound carbohydrate are opposite in sign to those of the free sugar and produce negative NOEs.[25] In the presence of excess ligand, NOEs between bound oligosaccharide protons appear as negative peaks on the averaged ligand resonances and give rise to cross-peaks with the same sign as the diagonal in pure phase absorption NOESY spectra. Following this methodology, the conformational changes that occur upon binding of **2** to ricin-B have been recently studied by us[15] employing TR-NOE experiments both in the laboratory and in rotating frames, TR-NOESY and TR-ROESY.[36] Summarizing, the results indicate that the bound conformation is slightly separated from the *exo*-anomeric position toward smaller Φ angles, while the orientation around the aglyconic bond is exclusively *syn*. The relevant interproton distances (H1′−H4 *ca.* 2.2−2.3 Å) are in agreement with those reported for the binding of deuterated methyl β-lactoside (**4**) to ricin-B in the pioneer work of Prestegard and co-workers.[16]

For *C*-lactose, the NOEs observed in the presence of ricin-B are negative, thus indicating ligand binding. The same was found for the regular disaccharides **2** and **4**. Two different ligands were used, free *C*-lactose and its β-methyl analogue (**3**). The use of **1** as a mixture of anomers, although it produced a large number of cross-peaks, was shown to be very convenient, since the chemical shifts of the conformationally relevant Glc H3 proton belonging to the α-species is fairly different from that belonging to the β-species, thus allowing this key NOE to be detected at two different proton frequencies. In addition, the blocked β-methyl anomer was also used to independently confirm the observations. The comparison between the NOESY spectra of **1** recorded in the absence (Figure 4a) and in the presence of the lectin (Figure 4c) shows important differences. First, the presence of both H1′/H3 and HproR/H6 cross-peaks, which define the population around minimum B, indicates that the *anti* conformation is indeed recognized by the protein, in contrast with the results obtained for methyl α- and β-lactosides, **2**[15] and **4**.[16] Second, a total of four NOEs, which were observed for free **1**, are not detected in the complex (Table 5): The H4/H2′ NOE (an exclusive NOE of the region around minimum C) is not present, indicating that this conformation is not bound. In addition, three NOEs that characterize the *syn* conformation (HproR/H3, HproS/H5, and HproS/H6, exclusive NOEs) are also absent in the TR-NOESY spectrum (Figure 4b). Therefore, and although mainly on the basis of the absence of these three NOEs (while those exclusive for the *anti* conformation are clearly present), the *syn* conformation does not seem to be appreciably bound by the lectin. It seems difficult to justify, given the small size of the ligand and the magnitude of the NOEs detected for the *anti* conformer, that the lack of detection of the key NOEs for the *syn* conformation in the presence of protein is merely a limitation of the NOE experiments. Indeed, the results point out that the *syn* conformation is not bound by the protein, at least in an important amount. The presence of the H1′/H4 cross-peak seems to be a contradiction. However, a careful study of the spectrum shows that, for the complex, the H1′/HproS NOE (*ca.* −3%) is much more intense than the H1′/H4 NOE (*ca.* −1%), while for free **1**, these cross-peaks have the same intensity. Since spin diffusion is extremely efficient for a molecular complex of this size, it may be that the H1′/H4 NOE is mediated by an indirect effect in the complex. Indeed, the presence of the two methylene protons in **1** provides important spin diffusion pathways, and therefore an indirect H1′/H4 cross-peak *via* HproS may be expected. Possible indirect transfers from H1′ to H4′ and to H6′ are also evident in the spectrum.[15,16] To confirm this hypothesis and to differentiate spin diffusion effects from direct NOE enhancements, the use of transferred NOE experiments in the rotating frame (TR-ROESY)[37,38] is essential, since under spin-locking conditions, direct and three-spin effects are of opposite sign. The major disadvantage of TR-ROESY is that cross-relaxation of the free ligand cannot be neglected and must be measured in a separate experiment.[39] Furthermore, due to the positive sign of the NOE cross-peaks, independently of the molecular size, it is not evident whether transfer NOE peaks for an exchanging protein/ligand system are observed. However, the cross-relaxation rates for small and for large molecules are different enough to be distinguished at moderately short mixing times.[38] This aspect led us to perform rotating frame TR-NOE experiments to compare the obtained results with those from the regular TR-NOESY experiments described above. A summary of the results is also given in Table 5. It is evident that spin diffusion is almost eliminated, since the indirect transfer from H1′ to H4′ and H6′ (mediated by H3′ and H5′) is produced with a change in the sign, and therefore these cross-peaks would appear with the same sign as the diagonal peaks or almost with zero intensity (supporting information). The experimental data also show that the H1′/H3 ROE is about 3 times higher in the spectrum recorded in the presence of protein than in the spectra for free

(36) Perlman, M. E.; Davis, D. G.; Koszalka, G. W.; Tuttle, J. V.; London, R. E. *Biochemistry* **1994**, *33*, 7547−7559.

(37) Bothner-By, A. A.; Stephens, R. L.; Lee, J.-M.; Warren, C. D.; Jeanloz, R. W. *J. Am. Chem. Soc.* **1984**, *106*, 811−813.

(38) Brown, L. R.; Farmer, B. T., II. *Methods Enzymol.* **1989**, *176*, 199−216.

(39) Arepalli, S. R.; Glaudemans, C. P. J.; Daves, G. D.; Kovac, P.; Bax, A. *J. Magn. Reson. B* **1995**, *106*, 195−198.

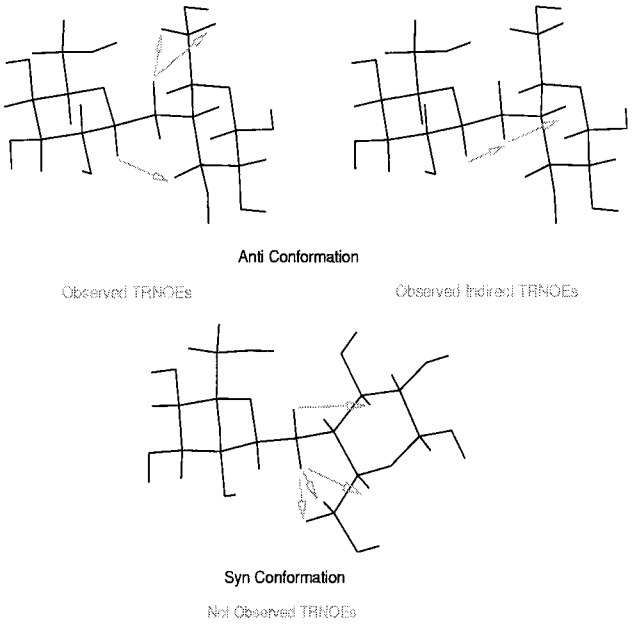

Figure 6. Summary of the observed and not observed NOE cross-peaks in the NOESY spectra carried out for the molecular complex of **1**/ricin-B (molar ratio of *C*-lactose/ricin-B, 20:1). The NOEs corresponding to the two major conformers of free **1** (*anti* and *syn*) are separated. In addition, the cross-peaks corresponding to spin difussion effects are also shown.

1 at the same mixing time. In contrast, the H1′/H4 NOE has the same magnitude in both cases, hence demonstrating that the corresponding TR-NOESY cross-peak, detected in the complex between **1** and the lectin, is mediated by an indirect effect. The presence of the H1′/H4 cross-peak in the TR-ROESY experiment is obviously due to the excess of free ligand. Differences between TR-NOESY and TR-ROESY spectra are also found for H1′/H4′, HproS/(H3′ + H5′), and HproR/(H3′ + H5′) cross-peaks, which disappear in the TR-ROESY spectrum (indirect effects mediated by H3′ + H5′ and H-1′, respectively). Our results confirm recent reports which indicate that spin diffusion plays a significant role in transferred NOE studies.[16,39] The NOESY experiments were repeated with the blocked *C*-lactoside analogue **3**. Basically the same results were found with this ligand (Table 5), which showed the same set of present and absent NOE cross-peaks, with H1′/H3, HproR/H6 and intraresidue intensities similar to those reported above for the α/β mixture of anomers. A quantitative analysis of the TR-NOE data obtained for *C*-lactose/ricin-B was attempted by simulation of the TR-NOESY spectra according to the full relaxation matrix method.[40] However, it was not possible to completely reproduce the experimental data by using a rigid model of the ligand within the binding site. It was observed that the correlation times for the bound state and the exchange-rate constants that fit all the intra-galactose NOEs did not reproduce all the intra- and interresidue NOEs involving the glucose unit. Therefore, the derivation of average distances cannot be performed in a quantitative way. On the other hand, for methyl α-lactoside/ricin-B all the experimental TR-NOEs could be fitted by using a simple set of parameters.[15] This fact is evidence that *C*-lactose is mobile even in the binding site, and that several conformers within the *anti* valley defined by minimum A are still possible.

More importantantly, the experimental TR-NOE results indicate (Figure 6), unequivocally and unexpectedly, that ricin-B preferentially selects different conformers of *C*-lactose, (**1** (*anti*)) and its *O*-analogue (**2** (*syn*)). Nevertheless, it has to be mentioned that conformational changes around glycosidic linkages have also been detected for carbohydrate ligands upon binding to proteins.[17,33]

Molecular Modeling. Crystallographic and binding studies of the ricin-B/lactose complex have shown that the lectin contains two noncooperative β-galactose -binding sites.[41] In order to make a qualitative estimation of the relative binding affinities of **1** and **2**, competitive TR-NOESY experiments, with different **1**:**2** ratios, were performed. It was observed that the increase in the amount of **2** added to the NMR tube induced a decrease in the negative NOE cross-peak intensities of **1**. When a 1:1 ratio was reached, the NOEs of *C*-lactose became positive, whereas strong negative NOEs were clearly observed for *O*-lactose. Two different conclusions can be drawn from these results: (a) both ligands compete for the same binding sites of the lectin and (b) the affinity constant of **1** is probably smaller than that of **2**.

Our previous studies using monodeoxy, *O*-methyl, halodeoxy, and other modified lactose derivatives[42] have shown that galactose HO-4, HO-3, and HO-6 are key polar groups in the interaction with ricin-B, while the glucose moiety, having the $^4C_1$ conformation, is important for recognition and binding, too. In particular, a non polar interaction involving the 3-position has been demonstrated to be operative.[42] In order to clarify the different behavior of **2** with respect to that of the synthetic analogue **1**, the galactose-binding subdomains of ricin-B, 1α and 2γ, were constructed from the crystallographic coordinates of ricin-B and subjected to independent energy minimization processes in the presence of **1** and **2**.[15] Thus, rigid residue and relaxed energy maps were constructed for the corresponding bimolecular complexes. The starting conformations of the sugars were those deduced from the TR-NOE studies, and the disaccharides were docked to match the hydrogen bond pattern observed in the crystal and deduced from the ligand-binding studies. The polypeptide backbone was held fixed, while the lateral chains were allowed to rotate freely during the minimizations. The obtained results are summarized in Figure 7. It can be observed that the polypeptide chain imposes an important constraint to the accessible torsion angles of **2**. Indeed, the *anti* region basically disappears, and only the central region of the map, somehow separated from the *exo*-anomeric position, seems to be energetically possible. In addition, there are significant van der Waals contacts between the glucose ring (mainly the C3 region) and amino acids of the polypeptide sequence, namely, Ala-237 (for subdomain 2γ) and Asp-25 and Arg-27 (for subdomain 1α). In fact, the major conformation in solution deduced for **2** would bring the C3 region of the lactoside and the mentioned amino acid residues into steric conflict. The lack of recognition of the *anti* conformation of **2** by the lectin could be explained by a steric interaction between the hydroxymethyl group of the glucose moiety and the protein.[15] Although the

(40) London, R. E.; Perlman, M. E.; D. G. *J. Magn. Reson.* **1992**, *97*, 79−98.

(41) (a) Monfort, W.; Villafranca, J. E.; Monzingo, A. F.; Ernst, S. R.; Katzin, B.; Rutenber, E.; Xuong, N. H.; Hamlin, R.; Robertus, J. D. *J. Biol. Chem.* **1987**, *262*, 5398−5403. (b) Rutenber, E.; Robertus, J. D. *Proteins* **1991**, *10*, 260−269. (c) Baenzinger, J. U.; Fiete, D. *J. Biol. Chem.* **1979**, *254*, 9795−9799. (d) Shimada, T.; Funatsu, G. *Agric. Biol. Chem.* **1985**, *49*, 2125−2130. (e) Houston, L. L.; Dooley, T. P. *J. Biol. Chem.* **1982**, *257*, 4147−4151. (f) Olsnes, S.; Pihl, A. In *The molecular actions of toxins and viruses*; Cohen, P., Van Heyningen, S., Eds.; Elsevier Biomedical Press: New York, 1982; pp 52−105. (g) Zentz, C.; Frenoy, J. P.; Bourillon, R. *Biochim. Biophys. Acta* **1978**, *536*, 18−26.

(42) (a) Rivera-Sagredo, A.; Solis, D.; Diaz-Mauriño, T.; Jiménez-Barbero, J.; Martín-Lomas, M. *Eur. J. Biochem.* **1991**, *197*, 217−228. (b) Solis, D.; Fernandez, P.; Diaz-Mauriño, T.; Jiménez-Barbero, J.; Martín-Lomas, M. *Eur. J. Biochem.* **1993**, *214*, 677−683. (c) Fernandez, P.; Jimenez-Barbero, J.; Martin-Lomas, M.; Solis, D; Diaz-Mauriño, T. *Carbohydr. Res.* **1994**, *256*, 223−244.

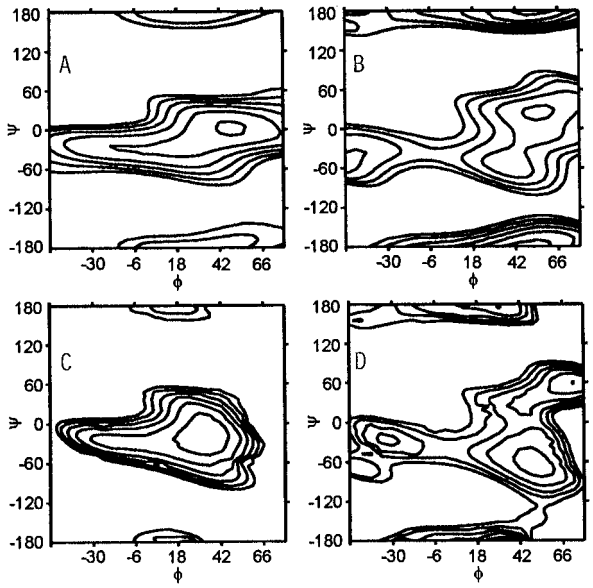

Figure 7. Rigid residue (A, B) and relaxed steric energy maps (C, D) of methyl α-lactoside (**2**) and *C*-lactose (**1**) carried out in the presence of the 1α-subdomain of ricin-B. Maps A and C correspond to compound **2** and maps B and D to compound **1**. The starting conformations corresponded to the global minimum geometries found for the free disaccharide and pseudo-disaccharide. The backbone atoms of the polypeptide chains were held fixed using the FIX option of INSIGHT II (Biosym Technologies). The lateral chains of the different amino acids were allowed to move freely during the protocol. A grid step of 5° was used. The CVFF force was employed. It can be observed that the *anti* region (bottom part of the maps) is forbidden for the ricin-B/**2** complex. On the other hand, no important restrictions are apparent for either the *syn* or *anti* region in the case of the ricin-B/**1** complex.

calculations should be taken with caution, since they are the product of a rough protocol, the deduced results are in complete agreement with our previous quantitative binding studies.[42] Therefore, and although the affinity of ricin-B resides more in the galactose residue, these results allow the higher affinity of ricin-B for lactose and larger oligosaccharides than for simple galactosides to be explained. However, from the results obtained for **1** (Figures 6 and 7), no unambiguous evidence could be taken as responsible for the different bound conformation of **1** with respect to that of **2**. In fact, the energy differences found between the *anti* region and the central *syn* region deduced for free **1** are basically maintained in the molecular complex. It is clear, however, that conformers within the *anti* region can still be recognized by ricin-B. Although merely speculative, the higher flexibility, as well as the larger distances between the pyranoid rings, might allow the recognition of the *anti* conformation of *C*-lactose. Nevertheless, no obvious reason has been found for the exclusive binding of this conformation to the protein (Figure 8).

Concluding Remarks. In conclusion, we have shown, for the first time, not only that the three-dimensional structure of a *C*-glycoside may be different from that of its corresponding *O*-glycoside in the free state, but also that a carbohydrate-binding protein may select different conformations of these types of compounds. Therefore, it seems necessary to consider, as is the case for other carbohydrate ligands, that conformational changes around glycosidic linkages are likely to occur upon binding to proteins.[17,33] Although the case presented here cannot be generalized, and it is evident that ricin-B is not a glycosidase, it seems that care should be taken when competitive inhibitors of glycosidases based on *C*-glycosides are designed, since these compounds may have preferred conformations different from those of their natural substrates. The next step will now be to deduce the conformation of a *C*-glycoside when bound to a glycosidase enzyme.

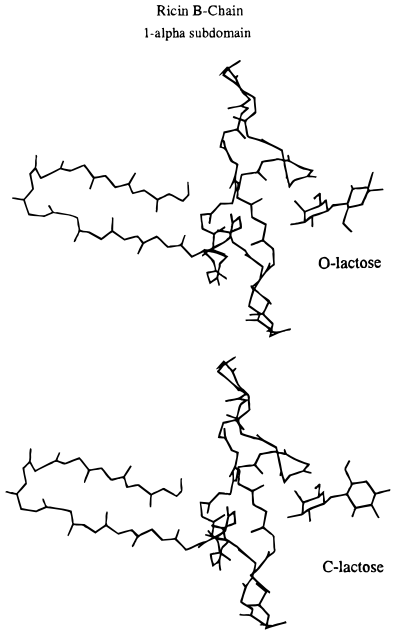

Figure 8. Compounds **1** and **2** were docked into the ricin-B 1α-subdomain, constructed from the crystallographic coordinates of ricin-B. Both ligands were docked to match the hydrogen bond pattern observed in the crystal for the galactose moiety. Extensive minimization of each complex with the CVFF program was performed.

Experimental Section

Materials. Compounds **1, 2,** and **3** were prepared as previously described. Compound **3** (methyl (4-*C*-2,6-anhydro-1-deoxy-D-glycero-L-mannoheptit-1-yl)-4-deoxy-β-D-glucopyranoside) was synthesized from **1** as follows: (a) pyridine, acetic anhydride (quantitative); (b) hydrazine acetate (1.4 equiv), DMF, room temperature, 1 h (90%); (c) trichloroacetonitrile (18 equiv), DBU, catalyst, dichloromethane, room temperature, 90 min (90%); (d) methanol (6 equiv), dry dichloromethane, $BF_3 \cdot Et_2O$ (0.1 M in dichloromethane, 0.1 equiv), 0 °C, 90 min (80%); (e) sodium methoxide, methanol, room temperature (quantitative). Details of the procedure will be reported elsewhere. The ricin-B chain was purchased from Sigma Chemical Co., St. Louis, MO.

Conformational Calculations. Molecular Mechanics and Dynamics for the Free Disaccharides. Glycosidic torsion angles are defined as Φ (H1′−C1′−Cα−C4) and Ψ (C1′−Cα−C4−H4). Relaxed (Φ, Ψ) potential energy maps were calculated for β-*C*-lactose (**1**) using MM3* ($\epsilon = 80$) as integrated in MACROMODEL 4.5.[43] Only the *gg* and *gt* conformers of the lateral chain of the glucose moiety and the *gt* and *tg* rotamers of the galactose one were taken into account, since they have been shown to be much more stable than the alternative *tg* and *gg* conformers, respectively.[24] Thus, four combinations were taken into account, namely, *gggt*, *gtgt*, *ggtg*, and *gttg*. The first two characters correspond to the glucose unit, and the other two to the galactose one. The starting position of the secondary hydroxyl groups was set as *c* (clockwise) or *r* (anticlockwise). Four combinations were used: *cc*, *cr*, *rc*, and *rr*. In total, 6400 conformers were calculated. The previous step involved the generation of the corresponding rigid residue maps by using a grid step of 18°. Then, every Φ, Ψ point of this map was optimized using 100 steepest descent steps, followed by 500 conjugate gradient iterations. The rms derivative in low-energy regions was smaller than 0.05 kJ mol^{-1} A^{-1}. Despite the restriction set around the glycosidic linkages (10 000 kJ/rad^2), deviations smaller than 0.3° in Φ and Ψ values were observed in high-energy regions. From these relaxed energy maps, adiabatic surfaces were built by

(43) Mohamadi, F.; Richards, N. G. J.; Guida, W. C.; Liskamp, R.; Caufield, C.; Chang, G.; Hendrickson, T.; Still, W. C. *J. Comput. Chem.* **1990**, *11*, 440−467.

choosing the lowest energy structure for a given Φ, Ψ point. Then, the probability distribution was calculated for each Φ, Ψ point according to a Boltzmann function.

The geometries describing the two main minima were extensively minimized using conjugate gradients and then taken as starting structures for molecular dynamics simulations by using MM3*, with the GB/SA solvent model.[44] The simulations were performed at 300 K with a time step of 1 fs. The equilibration time was 100 ps while the total simulation time was 3 ns. The temperature was controlled during the equilibration and simulation periods by coupling to a temperature bath, using an exponential decay constant of 0.1 ps[45] and the SHAKE option to keep C−H bonds fixed. During the equilibration period, the velocities were scaled when the difference between the actual and the required temperature was higher than 10°. Trajectory frames were saved every 0.5 ps.

Probability and NOE Calculations for the Free Disaccharides. From the relaxed energy maps, the probability distribution was calculated for each Φ, Ψ point. Assuming that the entropy difference among the different conformers is negligible, the probability P of a given Φ, Ψ point is[46]

$$P_{\Phi\Psi} = \Sigma_i\{\exp(-E_i/RT)\}/\Sigma_i\Sigma_{\Phi\Psi}\{\exp(-E_{i\Phi\Psi}/RT)\}$$

The conformational entropy S associated with the ensemble was estimated[46] as $S = -R\Sigma_i(p_i \text{ L n } p_i)$.

The estimated probability distributions were used to calculate the interproton average distances. Since the time scale of motion around the glycosidic linkages and hydroxymethyl lateral chains is not precisely known, both $\langle r^{-6}\rangle_{kl}$ and $\langle r^{-3}\rangle_{kl}$ averages were calculated:

$$\langle r^{-6}\rangle_{kl} = \Sigma P_{\Phi\Psi} r^{-6}_{kl(\Phi\Psi)}$$

$$\langle r^{-3}\rangle_{kl} = \Sigma P_{\Phi\Psi} r^{-3}_{kl(\Phi\Psi)}$$

The steady state 1D-NOEs were calculated according to the complete relaxation matrix by solving the simultaneous set of linear equations proposed by Noggle and Schrimer,[47] and using the average relaxation rates (from $\langle r^{-6}\rangle_{kl}$ and $\langle r^{-3}\rangle_{kl}$) calculated from the relaxed relative energies at 300 K. Isotropic motion and external relaxation of 0.1 s^{-1} were assumed in the calculations. Similar results were found for both types of averaging. Of course, this approach represents an oversimplification since both libration of the pyranoid rings and internal motion around the glycosidic linkages are taking place.[48] Since NOEs are extremely dependent on the correlation time, different τ_c values were used in order to obtain the best match between experimental and calculated NOEs for a given intraresidue proton pair. A τ_c value of 0.15 ns was used in order to obtain the best match between the experimental (Varian Unity 500) and the calculated NOEs for the intraresidue proton pairs H1′/H3′, H1′/H5′, and H4/H2 of **1**.

Vicinal coupling constants were calculated for each conformer of **1** using the Karplus−Altona equation.[27] Ensemble average values were calculated from the distribution according to: $J_i = \sum P_{\Phi\Psi} J_{i\Phi\Psi}$, and compared to the experimental (Bruker AMX 600) values.

Molecular Modeling of the Complex. Ricin-B coordinates were obtained from the crystal structure.[41b] The carbohydrate-binding domains 1α and 2γ were built from these coordinates. The galactose ring of compounds **1** and **2** was docked as to fit the hydrogen bond pattern both observed in the crystal structure and also deduced from ligand-binding studies. A biharmonic potential was used to satisfy these hydrogen bond distances during the calculations. No restrictions were set either around the glycosidic linkages or for the glucose rings, and the starting oligosaccharide conformations corresponded to the global minimum geometries found for the free disaccharide and pseudodisaccharide. The backbone atoms of the polypeptide chains were held fixed using the FIX option of INSIGHT II (Biosym Technologies). The lateral chains of the different amino acids were allowed to move freely during the protocol. The structures of the complexes built following this protocol were used to calculate rigid residue and relaxed energy maps as described above for the free molecules, but using only the previously deduced lowest energy orientation of the hydroxyl and hydroxymethyl groups. In this case, a shorter grid step (5°) was used. The CVFF force field[49] as implemented in the DISCOVER 2.9 program (Biosym Technologies) was employed.

NMR Experiments. NMR spectra of **1** were recorded in D_2O, on a Varian Unity 500 spectrometer. Proton chemical shifts were referenced to external acetone at $\delta = 2.225$ ppm. A Bruker AMX 600 machine was also used to measure the coupling constants of **1**. Carbon chemical shifts were referenced to external dioxane at $\delta = 67.4$ ppm. NMR spectra of **3** were also recorded in DMSO-d_6, DMF-d_6, and Py-d_5. DQF-COSY experiments were performed in the phase sensitive mode using the standard Varian sequence. The pure absorption one-bond proton−carbon correlation experiments were collected using the HMQC pulse sequences. A relaxation delay of 2 s and a delay corresponding to a J value of 152 Hz were used. A BIRD pulse was used to minimize the proton signals bonded to ^{12}C. ^{13}C-decoupling was achieved by the WALTZ scheme. The 2D rotating frame NOE (ROESY, CAMELSPIN) experiments were recorded in the phase sensitive mode. The spin-lock period consisted of a train of 30° pulses (2.5 μs), separated by delays of 50 μs. Mixing times of 250, 350, and 500 ms were employed. The rf carrier was set at $\delta = 6.0$ ppm to minimize spurious Hartmann−Hahn effects.[50a] Cross-peak intensities were corrected according to their offset.[50] No correction for Hartmann−Hahn transfers was performed.[50b] Prior to Fourier transformation, squared cosine bell functions were applied in both dimensions. The spectrum was integrated using standard Varian software after applying a third-order polynomial baseline correction in F_2.

The 2D-NOESY experiments were carried out with mixing times of 300, 500, and 700 ms. Thirty-two scans were used per increment with a relaxation delay of 2 s. Processing similar to that described for ROESY was applied. All 2D-NOE experiments were repeated twice and integrated using standard Varian software after applying a third-order polynomial baseline correction in F_2. Cross-relaxation rates were estimated by extrapolation to zero mixing time from the linear dependence of $I_{ij}/(I_{ii} \times \text{mixing time})$ *versus* mixing time, where I_{ij} and I_{ii} are the integrated volumes of the cross-peaks and diagonal peaks, respectively.[51]

The steady state NOEs were obtained through the interleaved differential technique using a saturation delay of 10 s. The experiment was repeated three times. Since the relevant protons for the NOE calculations are not affected by strong coupling, no effort was made to account for these effects.

Transferred NOE Experiments. TR-NOESY Experiments. The regular NOESY sequence was used with mixing times of 120, 200, 300, and 400 ms, for two different molar ratios of *C*-lactose/ricin-B (30:1 and 20:1) at 30 °C. A NOESY experiment (300 ms, 30 °C) was also performed with a 20:1 molar ratio of methyl β-*C*-lactoside/ricin-B. Samples of ricin-B were concentrated after exchange with deuterated sodium phosphate (20 mM) buffer in microconcentrators and transferred to the NMR tube to give a final pH of 6.5, uncorrected for isotope effects. A small amount of sodium azide was added too. The concentration of ricin-B (0.12 mM) within the NMR tube was measured with UV (extinction coefficient, $E^{1\%}$ (at 280 nm, 1 cm), of 14.9).[41] Line broadening of the galactose and glucose protons was monitored after the addition of ligands. The theoretical analysis of the TR-NOEs was attempted according to the full relaxation matrix as recently described[40] and as followed by us for the binding of **2** to ricin-B.[15] Thus, different correlation times for the bound state, τ_b, exchange-rate

(44) Still, W. C.; Tempczyk, A.; Hawley, R. C.; Hendrickson, T. *J. Am. Chem. Soc.* **1990**, *112*, 6127−6128.
(45) Berendsen, H. J. C.; Postma, J. P. M.; van Gunsteren. W. F.; Di Nola, A.; Haak, J. R. *J. Chem. Phys.* **1984**, *81*, 3684−3690.
(46) Cumming, D. A.; Carver, J. P. *Biochemistry* **1987**, *26*, 6664−6676.
(47) Noggle, J. H.; Schirmer, R. E. *The Nuclear Overhauser Effect: Chemical Applications;* Academic Press: New York, 1971.
(48) Hajduk, P. J.; Horita, D. A.; Lerner, L. E. *J. Am. Chem. Soc.* **1993**, *115*, 9196−9201.
(49) Hagler, A. T.; Lifson, P.; Dauber, P. *J. Am. Chem. Soc.* **1979**, *101*, 5122−5130.
(50) (a) Bax, A. Davis, D. G. *J. Magn. Reson.* **1985**, *63*, 207−213. (b) Bax, A *J. Magn. Reson.* **1988**, *77*, 134−147.
(51) (a) Van Halbeek, H.; Poppe, L. *Magn. Reson. Chem.* **1992**, *30*, S74−S86. (b) Macura, S.; Farmer, B. T., II; Brown, L. R. *J. Magn. Reson.* **1986**, *70*, 493−499.

constants, k, defined after London as $p_f k = k_{-1}$, and leakage relaxation times, ρ^*, were employed. Normalized intensity values were used to verify the matching.[40,51b] The τ_c for the free state of **1** was set to 0.15 ns. In particular, three correlation times for the bound state were tested, namely, 25, 32, and 50 ns. Exchange-rate constants, between 50 and 1000 s^{-1}, and external relaxation times for the bound state of 0.3, 1.0, and 3.0 s were used in different calculations. The best results for the galactose residue protons of **1** were obtained using a bound correlation time of 3 ns, and a $k = 200$ s^{-1}. However, these values did not reproduce all the interglycosidic TR-NOEs. In contrast, for **2**/ricin-B all the experimental TR-NOEs could be fitted by a simple set of parameters (correlation time 20−25 ns, and $k = 150-300$ s^{-1}).

TR-ROESY Experiments. The regular ROESY (CAMELSPIN) sequence used spin-locking times of 150, 250, and 350 ms. The spin-lock period consisted of a train of 30° pulses (2.5 μs), separated by delays of 50 μs. The rf carrier was set at $\delta = 6.0$ ppm to minimize spurious Hartmann−Hahn effects.[50a] Cross-peak intensities were corrected as described above.

Acknowledgment. Financial support by DGICYT (Grant PB93-0127) is gratefully acknowledged. J.L.A. thanks Europharma S. A. for a fellowship. We thank Dr. Solis and Dr. Diaz-Mauriño for helpful discussions.

Supporting Information Available: A listing including two tables with NMR chemical shifts for compounds **1** and **3**, figures containing relaxed energy plots obtained by MM3* for **1**, 2D-NOESY of **1** and trace through H-1′ of this spectrum, ^{1}H-NMR spectrum of free and ricin-bound **1**, 2D-TR-NOESY of **1** and trace through H-1′ of this spectrum, plots of the MD simulations of **1**, expansion of the hydroxylic proton region of **3** in DMSO, trace through H-1′ of the 2D-TR-ROESY spectrum of **1**, 2D-TR-NOESY of **3**, and two expansions of this spectrum (17 pages). See any current masthead page for ordering and Internet access instructions.

JA9603463